Provided for non-commercial research and educational use only.
Not for reproduction or distribution or commercial use.

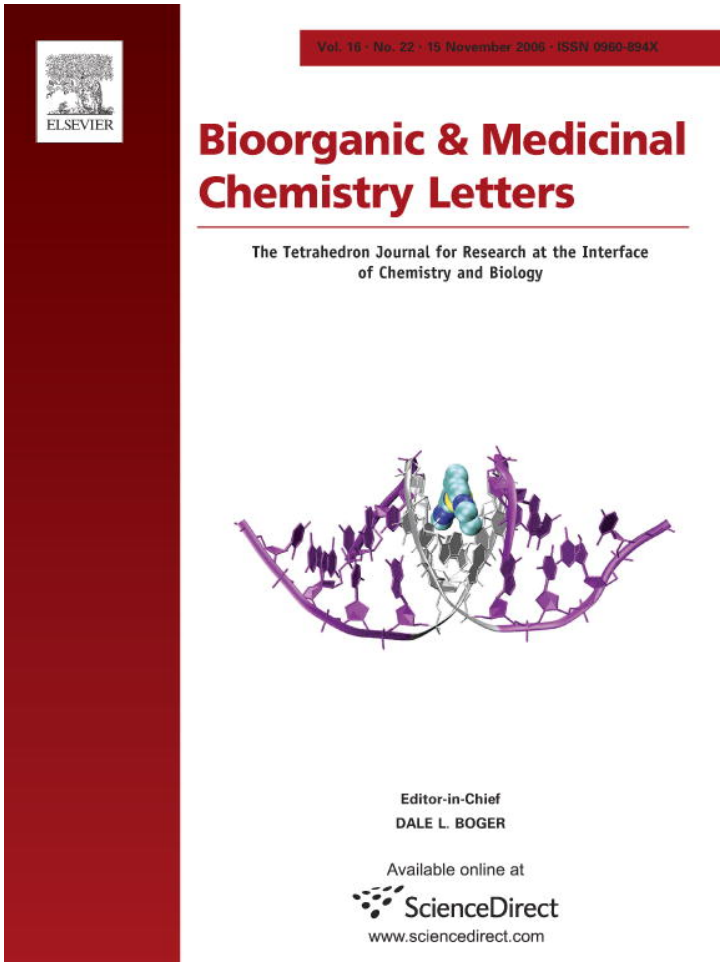

This article was originally published in a journal published by Elsevier, and the attached copy is provided by Elsevier for the author's benefit and for the benefit of the author's institution, for non-commercial research and educational use including without limitation use in instruction at your institution, sending it to specific colleagues that you know, and providing a copy to your institution's administrator.

All other uses, reproduction and distribution, including without limitation commercial reprints, selling or licensing copies or access, or posting on open internet sites, your personal or institution's website or repository, are prohibited. For exceptions, permission may be sought for such use through Elsevier's permissions site at:

http://www.elsevier.com/locate/permissionusematerial

Available online at www.sciencedirect.com
ScienceDirect
Bioorganic & Medicinal Chemistry Letters
ELSEVIER
Bioorganic & Medicinal Chemistry Letters 16 (2006) 5902–5906

Discovery of potent inhibitors of pseudomonal quorum sensing via pharmacophore modeling and in silico screening

Mutasem O. Taha,* Amal G. Al-Bakri and Waleed A. Zalloum

Faculty of Pharmacy, University of Jordan, Amman, Jordan

Received 14 May 2006; revised 10 August 2006; accepted 10 August 2006
Available online 30 August 2006

Abstract—HipHop-Refine was employed to derive a binding hypothesis for pseudomonal quorum sensing (QS) antagonists. The model was employed as 3D search query to screen the National Cancer Institute (NCI) database. One of the hits illustrated nanomolar QS inhibitory activity. The fact that this compound contained tetravalent lead (Pb) prompted us to evaluate the activities of phenyl mercuric nitrate and thimerosal, both fit the binding pharmacophore. The two mercurials illustrated nanomolar to low micromolar IC_{50} inhibitory values against pseudomonal QS. The three compounds represent a new class of QS inhibitors.
© 2006 Elsevier Ltd. All rights reserved.

Quorum sensing (QS) is a cell-density-dependent intercellular signaling mechanism that enables bacteria to coordinate the expression of certain genes.[1–9,40]

Gram negative bacteria rely on small auto-inducer (AI) molecules (e.g., acyl homoserine lactones, AHL) for their cell signaling.[7–9] The QS signaling of *P. aeruginosa* regulates a group of virulence factors that facilitate the establishment of infection, for example, pyoverdin and pyocynin.[9] There are two QS systems in *P. aeruginosa*: the Las and Rhl systems.[2] The Las system consists of LasR transcriptional regulator and LasI synthase protein. LasI is essential for the production of AI signal molecule, which is required by LasR to become active transcription factor.[7,8,10,11] The Rhl system seems to be regulated by the Las system.[12,13]

The great recent interest in developing new QS inhibitors as potential agents for reducing bacterial virulence,[1–6] combined with the lack of crystallographic structure for LasR, prompted us to develop a pharmacophoric model for LasR-based QS inhibitors. The model was subsequently utilized as 3D search query to screen the NCI database for possible QS inhibitors.

We employed the HipHop-Refine module of CATALYST software to build a plausible binding hypothesis. CATALYST models ligand–receptor interaction using information derived only from the ligand structure.[14–16] Molecules are described as collection of chemical functionalities arranged in 3D space. The conformational flexibility of training ligands is modeled by creating multiple conformers, judiciously prepared to emphasize representative coverage over a specified energy range. HipHop-Refine identifies a set of chemical features common to the most potent training molecules. This 3D array of chemical features provides a relative alignment for each input molecule consistent with their binding to a proposed common receptor site. The chemical features considered can be hydrogen bond donors and acceptors (HBDs and HBAs), aliphatic and aromatic hydrophobes, positive and negative charges, positive and negative ionizable groups and aromatic planes. However, HipHop-Refine utilizes the conformational space of inactive molecules to construct excluded volumes that represent the steric constraints of the proposed receptor.[17,18] Many CATALYST-derived models have been generated and used as queries for database searching.[19–23]

In this project, we employed four brominated furanones as training set for pharmacophore modeling (Fig. 1). This set of analogues represents a highly active anti-QS family that inhibit QS in several bacterial strains, probably via similar mechanism, that is, inhibition of QS transcription factors.[24–30,40] Despite that many brominated furanones were reported to have anti-QS

Keywords: HipHop-Refine; Pseudomonal quorum sensing antagonists; Tetravalent lead; Phenyl mercuric nitrate; Thimerosal.
* Corresponding author. Tel.: +00962 6 5355000x2505; fax: +00962 6 5339649; e-mail: mutasem@ju.edu.jo

0960-894X/$ - see front matter © 2006 Elsevier Ltd. All rights reserved.
doi:10.1016/j.bmcl.2006.08.069

Author's personal copy

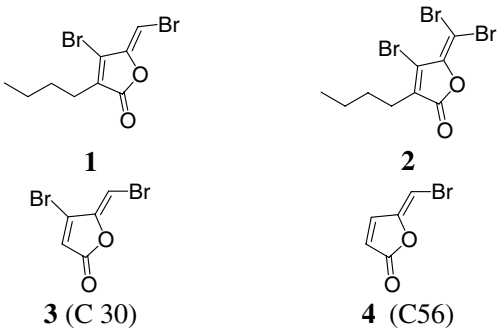

Figure 1. The structures of the training compounds.

activities, only few were found to be active specifically against pseudomonal QS, prompting us to limit our training set to **1**–**4**.[24–30,40,41] Furthermore, SAR studies of other classes of pseudomonal QS inhibitors suggest that brominated furanones function via distinct binding site(s).[40] For example, sulfur containing AHL analogues with long hydrophobic tails (C10 and C12) were found to have potent anti-LasR-based QS.[24,40] On the other hand, only furanones with short (or no) hydrophobic side chains are active pseudomonal QS inhibitors, suggesting they bind to a tighter binding pocket.[40,41] Therefore, we excluded other classes of inhibitors (other than halogenated furanones) from modeling.

The conformational space of each inhibitor was sampled utilizing the poling algorithm of CATALYST, which promotes conformational variation via employing molecular mechanical force field algorithm that penalizes similar conformers.[31–33] For each of the training compounds, a conformational database was generated using the 'best' option and default CATALYST conformation generation parameters (a maximum of 250 conformers and an energy range of 20 kcal/mol).[31–33]

Obviously, inhibitors **3** and **4** are rigid structures (one conformer for each), while the butyl tails of **1** and **2** render them more flexible (their numbers of conformers are 15 and 18, respectively).

After several preliminary trials, it was decided to configure HipHop-Refine as follows. Furanone **3**, which was reported to exert potent inhibitory actions against LasR-based pseudomonal QS (IC_{50} = 2.0 μM, in vitro data),[24,25,28] was assigned a Principal value of 2 to ensure that all of the chemical features in the compound will be considered in building the pharmacophore space.[17,18] On the other hand, compound **4**, which was reported to be 17 times less active than **3** (in vivo data),[28] was assigned a Principal value of 1 to ensure that its features will be considered when generating hypotheses and that it will be mapped at least once by each generated hypothesis.[17,18] However, **4** was allowed to miss one feature in any generated model by assigning it a MaxOmitFeat parameter of one.[17,18] Compounds **1** and **2** were qualitatively reported to be of minimal inhibitory activities against pseudomonal LasR (despite their potent actions against QS of other bacterial strains),[25,40,41] and therefore they were considered inactive by assigning them Principal values of zero.[17,18] However, based on the assumption that **1** and **2** are inactive due to their butyl tails, which seem to clash with certain steric boundaries within the binding site, they were assigned MaxOmitFeat values of zero. This value instructs HipHop-Refine to force the two inactive compounds to map all the pharmacophoric features of the binding model in order to identify spaces occupied by the two inactive compounds and free from the active inhibitors (i.e., **3** and **4**). These regions are subsequently filled with excluded volumes.

Finally, the software was configured to allow a minimal inter-feature distance of 10 pm to generate hypothesis that reflected the small size of the inhibitors.

These settings yielded one pharmacophore hypothesis comprised of two HBAs, two hydrophobic features, and seven excluded volumes (Fig. 3). Figure 4 shows overlay alignment of the training compounds onto the generated pharmacophore model.

We employed this model as 3D-search query against the NCI structure database (238,819 compounds) using the 'fast flexible search' approach implemented within CATALYST. However, before conducting the 3D search we reduced the database to 219,240 structures by removing compounds of molecular weights >500D and <100D to conform to the molecular size of active brominated furanones. The pharmacophore captured 86,001 hits. Hits are defined as those compounds that possess chemical functionalities that spatially overlap with corresponding features within the pharmacophoric model. The hits were subsequently fitted against the pharmacophore (see the fit equation in the footnote of Table 1) and the highest ranking 40 compounds were requested from the NCI. However, only 19 hits were actually available from the NCI and evaluated as QS inhibitors.[34,35] Their anti-QS activities were assessed through their effects on pseudomonal production of pyocyanin and pyoverdin.[24,36,37] Table 1 shows the NCI codes, fit values, and biological activities of some of the tested hits, while Figure 2 shows their corresponding chemical structures.

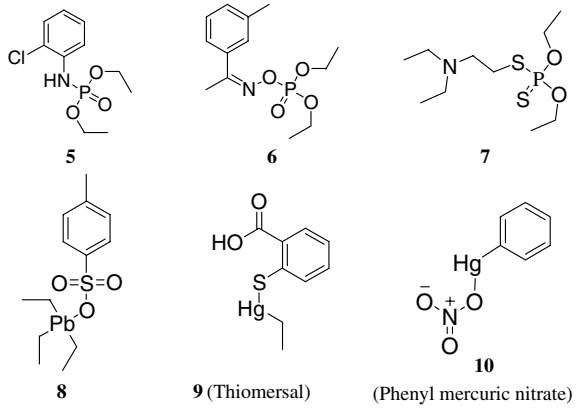

Figure 2. The structures of some evaluated in silico hits.

Author's personal copy

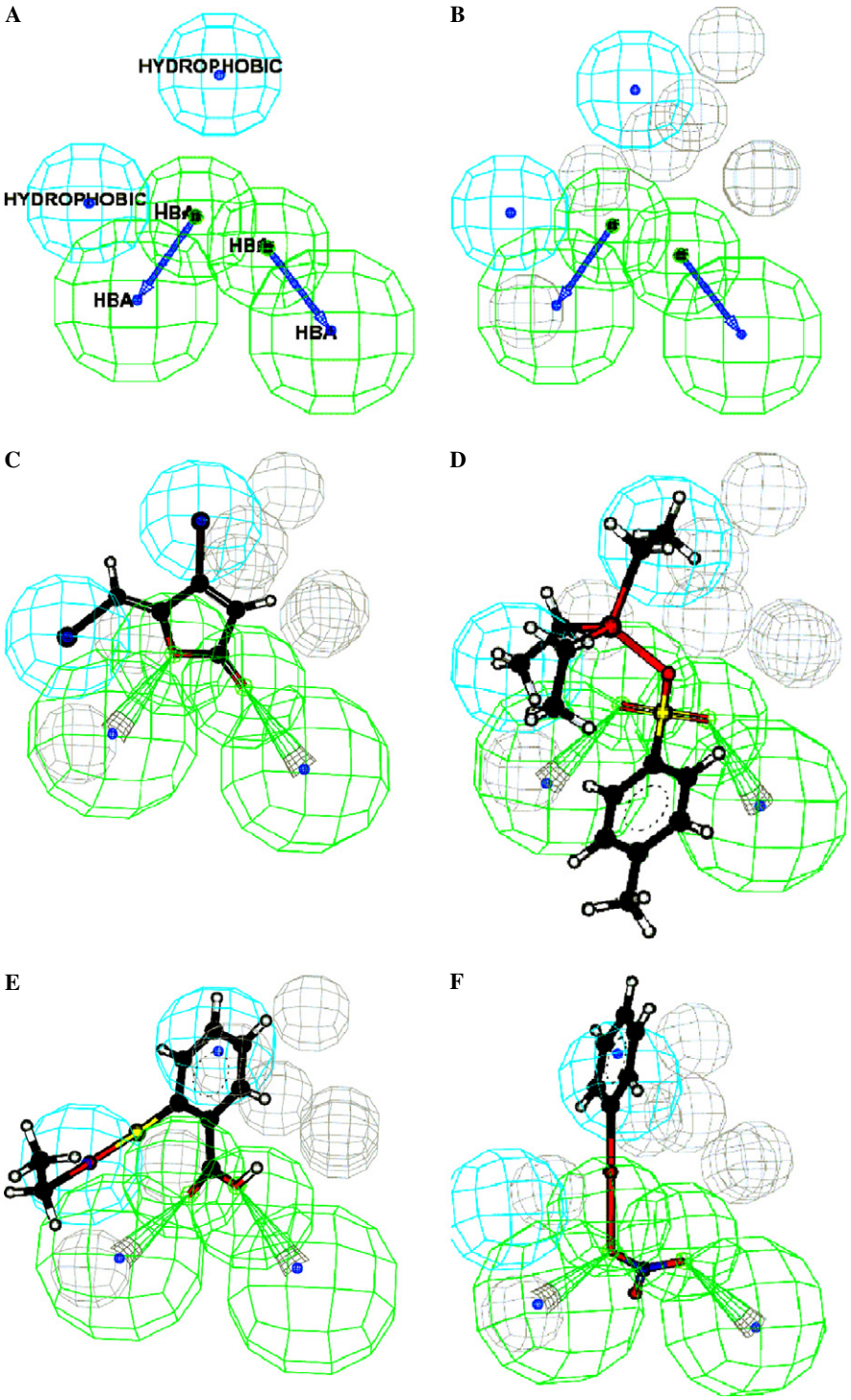

Figure 3. (A) Pharmacophore features, (B) with added excluded volumes (gray spheres). Mapping against (C) **3**, (D) **8**, (E) **9** and (F) **10**.

Most of the tested hits were inactive. However, one of the hits illustrated impressive QS inhibition, that is, **8** (IC_{50} values < 800 nM, Table 1 and Figs. 2 and 3D). This contradiction is quite intriguing, since the tested hits illustrated similar fit values against the pharmacophore. This conduct prompted us to suspect that the inhibitory action of **8** is related to the lead atom and mediated by an additional mechanism that complements pharmacophore recognition within the binding pocket of LasR. Two possible mechanisms were considered, namely, (i) nonspecific (promiscuous) inhibition[38] and (ii) active-site directed irreversible inhibition.

Tetravalent lead is known to form stable complexes with thiol (R–SH) groups,[39] and thus, it can act as a non-specific bacterial toxicant against variety of targets. However, the fact that **8** was devoid of any antibacterial actions within its anti-QS concentration range casts doubt on this mechanism. The promiscuous inhibition theory was further weakened by the

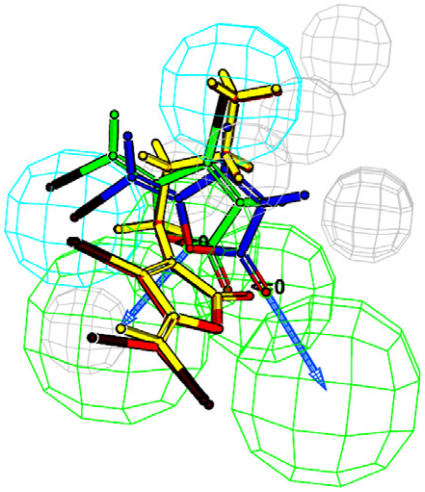

Figure 4. Overlay alignment of the training compounds: **1** (yellow), **2** (red), **3** (green) and **4** (blue) onto the generated pharmacophore model.

fact that tetraethyl-lead ($Pb(CH_2CH_3)_4$), which does not fit the pharmacophore, exhibited trivial anti-QS actions.

The fact that mercury and lead have similar chemical reactivities and biological profiles[39] prompted us to evaluate the anti-QS actions of two known mercurial biocides: thimerosal and phenyl mercuric nitrate (**9** and **10**, respectively, Fig. 2). Luckily, both compounds fitted tightly onto the pharmacophoric model (Table 1, Figs. 3E and 3F). Unsurprisingly, the two mercurials exhibited significant QS inhibitory actions (Table 1). Furthermore, they were devoid of any antibacterial activities within their QS inhibitory ranges. Interestingly, the fit values of **8**–**10** against the pharmacophoric model correlate well with their anti-QS activities (Table 1).

The fact that **8**–**10** combine the ability to fit onto the binding pharmacophore and to form stable covalent complexes with thiol groups strongly supports the active site-directed irreversible inhibition proposition, that is, initial selective and reversible binding within the binding pocket (i.e., pharmacophore recognition) followed by covalent bonding that connects certain nucleophilic center within the binding pocket (probably a thiol group) with the metallic core of the inhibitors.

Further evidence on the validity of this mechanism comes from investigating the effects of variable concentrations of QS auto-inducers (*N*-acyl homoserine lactones) on the production of pyocyanin and pyoverdin in the presence and absence of **8**. The presence of **8** inhibited the production of pyocyanin and pyoverdin regardless of the level of the added auto-inducers. On the other hand, absence of **8** allowed dramatic increase in the production of pyoverdin and pyocyanin in response to the added auto-inducers.

Finally, it remains to be mentioned that none of the compounds **8**–**10** altered the color intensity of pyoverdin or pyocyanin upon mixing and incubation overnight. Therefore, one can assume that the dramatic reduction in the color intensity of pyocynin and pyoverdin in the presence of **8**–**10** is most probably due to the inhibition of LasR and not simple chemical degradation or interaction.

Our results suggest that furanones **3** and **4** inhibit pseudomonal QS via an analogous mechanism, that is, active-site-directed irreversible inhibition, probably mediated by their Michael acceptor functionalities and bromo good leaving groups.

We believe the reason for the poor QS inhibitory actions of reversible binders (e.g., other screening hits and lactone analogues[24]) is related to the nanomolar affinities of the natural QS auto-inducers (AHL) to LasR,[30] which seem to expel and replace reversible binders within the binding pocket.

Table 1. The results of some evaluated in silico hits

Hits[a]	NCI code or chemical name	Best Fit values[b]	IC_{50} Assay (μM)	
			Pyocyanin	Pyoverdin
5	43465	3.27	N/A[c]	N/A
6	132963	3.74	N/A	N/A
7	133009	3.21	N/A	N/A
8	203113	3.90	0.282[d] (0.158[e])	0.355[d] (0.794[e])
9	Thimerosal	3.70	0.708[d] (3.162[e])	0.603[d] (3.166[e])
10	Phenyl mercuric nitrate[f]	2.50	3.019[d] (3.236[e])	3.162[d] (3.981[e])

[a] The compounds and their numbers are as in Figure 2.

[b] Fit values against the pharmacophore, calculated as in the following: Fit = Σmapped hypothesis features × W [1−Σ (disp/tol)^2], where Σmapped hypothesis features is the number of pharmacophore features that successfully superimpose corresponding chemical moieties within the fitted compound, W is the weight of the corresponding hypothesis feature spheres. This value is fixed to 1.0 in HipHop-generated models. disp is the distance between the center of a particular pharmacophoric sphere and the center of the corresponding superimposed chemical moiety of the fitted compound; tol is the radius of the pharmacophoric feature sphere (known as Tolerance, equals 1.6 Å by default). Σ(disp/tol)^2 is the summation of (disp/tol)^2 values for all pharmacophoric features that successfully superimpose corresponding chemical functionalities in the fitted compound.[18]

[c] Not active.

[d] IC_{50} against a pseudomonal clinical isolate from Jordan University Hospital, each value is the average of three trials.

[e] IC_{50} against a lab strain (ATCC: 9027), each value is the average of three trials.

[f] Mapping against the pharmacophore misses one feature.

Author's personal copy

Acknowledgment

The authors thank the National Cancer Institute (NCI) for kindly providing the tested hits.

References and notes

1. Geske, G. D.; Wezeman, R. J.; Siegel, A. P.; Blacwell, H. E. *J. Am. Chem. Soc* **2005**, *127*, 12762.
2. Smith, R. S.; Iglewski, B. H. *J. Clin. Invest.* **2003**, *112*, 1460.
3. Welch, M.; Dutton, J. M.; Glansdorp, F. G.; Thomas, G. L.; Smith, D. S.; Coulthurst, S. J.; Barnard, A. M. L.; Salmond, G. P. C.; Spring, D. R. *Bioorg. Med. Chem. Lett.* **2005**, *15*, 4235.
4. Zhao, G.; Wan, W.; Mansouri, S.; Alfaro, J. F.; Bassler, B. L.; Cornell, K. A.; Zhou, Z. S. *Bioorg. Med. Chem. Lett.* **2003**, *13*, 3897.
5. Scott, R. J.; Lian, L-Y.; Muharram, S. H.; Cockayne, A.; Wood, S. J.; Bycroft, B. W.; Williams, P.; Chan, W. C. *Bioorg. Med. Chem. Lett.* **2003**, *13*, 2449.
6. March, J. C.; Bentley, W. E. *Curr. Opin. Biotech.* **2004**, *15*, 495.
7. Pearson, J. P. *J. Bacteriol.* **2002**, *184*, 2569.
8. Pearson, J. P.; Passador, L.; Iglewski, B. H.; Greenberg, E. P. *Proc. Natl. Acad. Sci. U.S.A.* **1995**, *92*, 1490.
9. Rumbaugh, K. P.; Griswold, J. A.; Hamood, A. N. *Microbes Infect.* **2000**, *2*, 1721.
10. Donabedian, H. *J. Infect.* **2003**, *46*, 207.
11. Kiratisin, P.; Tucker, K. D.; Passador, L. *J. Bacteriol.* **2002**, *184*, 4912.
12. Latifi, A.; Foglino, M.; Tanaka, K.; Williams, P.; Lazdunski, A. *Mol. Microbiol.* **1996**, *21*, 1137.
13. Pesci, E. C.; Pearson, J. P.; Seed, P. C.; Iglewski, B. H. *J. Bacteriol.* **1997**, *179*, 3127.
14. Kurogi, Y.; Güner, O. F. *Curr. Med. Chem.* **2001**, *8*, 1035.
15. Sprague, P. W.; Hoffmann, R. In *Computer Assisted Lead Finding and Optimization—Current Tools for Medicinal Chemistry*; Van de Waterbeemd, H., Testa, B., Folkers, G., Eds.; VHCA: Basel, 1997; p 230.
16. Barnum, D.; Greene, J.; Smellie, A.; Sprague, P. *J. Chem. Inf. Comput. Sci.* **1996**, *36*, 563.
17. The 9th European CATALYST User Group Meeting, Advanced Seminars in CATALYST, Frankfurt, Germany, March 24, Accelrys Inc.: San Diego, CA, 2006.
18. Catalyst User Guide, Accelrys Software Inc., San Diego, 2005.
19. Greenidge, P. A.; Carlson, B.; Bladh, L.; Gillner, M. *J. Med. Chem.* **1998**, *41*, 2503.
20. Langer, T.; Hoffmann, R. D. *J. Chem. Inf. Comput. Sci.* **1998**, *38*, 325.
21. Karki, R. G.; Kulkarni, V. M. *Eur. J. Med. Chem.* **2001**, *36*, 147.
22. Singh, J.; Chuaqui, C. E.; Boriack-Sjodin, P. A.; Lee, W-C.; Pontz, T.; Corbley, M. J.; Cheung, H.-K.; Arduini, R. M.; Mead, J. N.; Newman, M. N.; Papadatos, J. L.; Bowes, S.; Josiah, S.; Ling, L. E. *Bioorg. Med. Chem. Lett.* **2003**, *13*, 4355.
23. Taha, M. O.; Qandil, A. M.; Zaki, D. D.; AlDamen, M. A. *Eur. J. Med. Chem.* **2005**, *40*, 701.
24. Persson, T.; Hansen, T. H.; Rasmussen, T. B.; Skindersø, M. E.; Givskov, M.; Nielsen, J. *Org. Biomol. Chem.* **2005**, *3*, 253.
25. Suga, H.; Smith, K. M. *Curr. Opin. Chem. Biol* **2003**, *7*, 586.
26. Kaplan, J. B. *Expert Opin. Ther. Pat.* **2005**, *8*, 955.
27. Ren, D.; Zuo, R.; Wood, T. K. *Appl. Microbiol. Cell. Physiol.* **2005**, *66*, 689.
28. Wu, H.; Song, Z.; Hentzer, M.; Andersen, J. B.; Molin, S.; Givskov, M.; Høiby, N. *J. Antimicrob. Chemother.* **2004**, *53*, 1054.
29. Smith, K. M.; Bu, Y.; Suga, H. *Chem. Biol.* **2003**, *10*, 81.
30. Passador, L.; Tucker, K. D.; Rguertin, K.; Journet, M. P.; Kende, A. S.; Iglewski, B. H. *J. Bacteriol.* **1996**, *178*, 5995.
31. Li, H.; Sutter, J.; Hoffmann, R. In *Pharmacophore Perception, Development, and Use in Drug Design*; Güner, O. F., Ed.; International University Line: California, 2000; p 173.
32. Smellie, A.; Teig, S.; Towbin, P. *J. Comput. Chem.* **1995**, *16*, 171.
33. Smellie, A.; Kahn, S. D.; Teig, S. L. *J. Chem. Inf. Comput. Sci.* **1995**, *35*, 285.
34. Briefly, bacterial cells were grown overnight in Oxoid nutrient broth. Cells were harvested by centrifugation for 10 min at 5000**g**. The resulting pellet was re-suspended in fresh sterile nutrient broth (10 mL) and diluted to an optical density of 0.05 at 600 nm (OD600)[35]. Thereafter, it was allowed to grow until mid-log phase (OD600 of 0.3–0.5). The cultures were then diluted to OD600 = 0.05 with fresh sterile nutrient broth (ca. to 300 mL) and aliquoted (18 mL) into sterile 100 mL conical flasks containing appropriate amounts of the tested compound(s) dissolved in sterile distilled water (2.0 mL) to achieve 50.00, 25.00, 10.00, 5.00, 2.50, 1.00, 0.10 or 0.001 μM and zero overall concentrations. The mixtures were subsequently shaken and incubated for 18 h at 37 °C. A 1.0 mL quantity was withdrawn from each culture to count the viable cells within the medium. The remaining culture medium was centrifuged for 30 min at 5000**g** to harvest bacterial cells. The resulting pellet was re-suspended in nutrient broth (10 mL) and the OD600 of this suspension was measured and utilized to normalize the absorbencies of pyocyanin and pyoverdin per bacterial optical density unit at 600 nm. To evaluate pyoverdin production, the absorbance of a 1.0-mL volume of the supernatant was measured at 405 nm using fresh nutrient broth as a blank. However, for the evaluation of pyocyanin production, the supernatant was extracted with chloroform (18 mL), and the extract was re-extracted by hydrochloric acid (4.0 mL, 0.2 N). The absorbencies of the HCl extracts were recorded at 520 nm.
35. Lawrence, J. V.; Maier, S. *Appl. Environ. Microbiol.* **1977**, *33*, 482.
36. Meyer, J. M.; Neely, A.; Stintzi, A.; Georges, C.; Holder, I. A. *Infect. Immun.* **1996**, *64*, 518.
37. Stintzi, A.; Evans, K.; Meyer, J.-M.; Poole, K. *FEMS Microbiol. Lett.* **1998**, *166*, 341.
38. McGovern, S. L.; Caselli, E.; Grigorieff, N.; Shoichet, B. K. *J. Med. Chem.* **2002**, *45*, 1712.
39. Vallee, B. L.; Ulmer, D. P. *Annu. Rev. Biochem.* **1972**, *41*, 91.
40. Rasmussen, T. B.; Givskov, M. *Int. J. Med. Microbiol.* **2006**, *296*, 149.
41. Hentzer, M.; Riedel, K.; Rasmussen, T. B.; Heydorn, A.; Andersen, J. B.; Parsek, M. R.; Rice, S. A.; Eberl, L.; Molin, S.; Hoiby, N.; Kjelleberg, S.; Givskov, M. *Microbiology* **2002**, *148*, 87.

Author's personal copy